

# Autoionization dynamics in the valence-shell photoionization spectrum of CO

J. E. Hardis, T. A. Ferrett, S. H. Southworth, and A. C. Parr  
*National Bureau of Standards, Gaithersburg, Maryland 20899*

P. Roy  
*Los Alamos National Laboratory, Los Alamos, New Mexico 87545*

J. L. Dehmer and P. M. Dehmer  
*Argonne National Laboratory, Argonne, Illinois 60439*

W. A. Chupka  
*Sterling Chemistry Laboratory, Yale University, New Haven, Connecticut 06511*

(Received 22 February 1988; accepted 25 March 1988)

Autoionizing Rydberg series in the valence-shell spectrum of CO have been studied by determining the high resolution relative photoionization cross section of cooled CO in the energy region 14.0–20.0 eV and by determining the vibrational branching ratios and the photoelectron angular distributions for production of  $\text{CO}^+ X^2\Sigma^+, v^+ = 0-2$  in the energy region 16.75–18.75 eV. Of particular interest are three prominent spectral features between 17.0 and 17.5 eV that result from interactions involving Rydberg series converging to the excited  $A^2\Pi$  and  $B^2\Sigma^+$  states of the ion. The results are discussed in the context of recent two-step multichannel quantum defect theory calculations by Leyh and Raseev (the following paper).

## I. INTRODUCTION

Autoionization of Rydberg states converts energy stored in the excited ion core into the ionization energy of the Rydberg electron. In molecules, this energy can be stored in a variety of modes—rotational, vibrational, electronic, and spin-orbit—and must be transferred to the Rydberg electron during a collision with the ion core. Consequently, molecular autoionization is a very useful means of studying basic molecular interactions involving the exchange of energy and angular momentum among electronic and nuclear modes. The effects of autoionization are prominent in numerous observables; however, of particular interest here is the progress in angle-resolved photoelectron studies using synchrotron radiation, which has made it possible to record photoelectron branching ratios and angular distributions with sufficient spectral resolution to clearly display the effects of autoionization. These quantities contain detailed dynamical information, and thus they provide an important test of our current understanding of molecular photoionization.<sup>1-4</sup>

One important theoretical approach in this context has been the multichannel quantum defect theory (MQDT),<sup>3</sup> which treats the interactions among entire channels in terms of a small number of parameters that characterize the short range interactions in the molecular core. This approach has been extremely successful in accounting for the observable effects of rotational and vibrational autoionization<sup>3,5-11</sup> and predissociation<sup>3,7,12</sup> in molecular hydrogen. The extension of MQDT analyses to more complex molecules<sup>13-16</sup> has also met with considerable success, but has been much more difficult and, at times, less definitive. For example, the MQDT treatment of electronic autoionization of the Hopfield series

in  $\text{N}_2$  was found to involve many more input parameters than were needed for  $\text{H}_2$ .<sup>13</sup> Accordingly, a two-step MQDT approach was used<sup>17,18</sup> in which the input parameters such as quantum defects and transition strengths were determined by *ab initio* calculations rather than by analysis of spectral data as was done for  $\text{H}_2$ . The results agreed qualitatively with experiment and provided significant insight into electronic autoionization in  $\text{N}_2$ .

A logical next step toward understanding more complex molecules is the characterization of autoionization in the valence-shell spectrum of CO. This step might be expected to be straightforward, since CO is isoelectronic with  $\text{N}_2$  and it differs from  $\text{N}_2$  mainly in the loss of inversion symmetry. Indeed, the initial two-step MQDT calculation<sup>19</sup> showed many similarities with the experimentally determined partial photoionization cross sections.<sup>20</sup> However, the calculations failed to account for a broad spectral feature at  $\sim 721 \text{ \AA}$  (17.2 eV) and produced a photoelectron asymmetry parameter for the intense  $3p\pi, v' = 0$  resonance at  $725.51 \text{ \AA}$  (17.09 eV) that appeared to differ significantly from fragmentary data.<sup>21</sup> These differences have stimulated new experimental and theoretical work.

This paper describes the measurements of the relative photoionization cross section for valence-shell photoionization of CO and the vibrational branching ratios and photoelectron angular distributions for the  $\text{CO}^+ X^2\Sigma^+, v^+ = 0-2$  ionization channels. All data were determined on a fine energy mesh with high resolution in order to provide an unambiguous experimental test of the corresponding theoretical quantities. This also eliminates the possibility that the previous disagreement between theory and experiment was due to an energy misalignment in a region of complex structure. A companion paper by Leyh and Raseev<sup>22</sup> describes significant advances in the two-step MQDT calculations.

## II. EXPERIMENT

### A. Photoionization cross section

The relative photoionization cross section for CO was determined in the region 600–890 Å (14.0–20.0 eV) using a high resolution photoionization mass spectrometer.<sup>23</sup> Briefly, the apparatus consisted of a helium continuum light source, a 3 m near normal incidence monochromator that dispersed and then refocused the selected light into an ionization chamber that was cooled to liquid nitrogen temperature, a set of ion extraction and focusing lenses, and a quadrupole mass spectrometer for ion detection. The monochromator was equipped with a 1200 line/mm, MgF<sub>2</sub>-coated aluminum grating blazed for 1300 Å in first order. For the present study, data were taken in first order using 25 μm entrance and exit slits, which resulted in an observed resolution of 0.07 Å. The results are shown in Fig. 1. The spectrum is dominated by autoionizing Rydberg series that converge to the  $A^2\Pi$  and  $B^2\Sigma^+$  states of the ion; the classification and identification of these series are reviewed in Sec. III A. Very weak features converging to excited vibrational levels of the  $X^2\Sigma^+$  ground state of the ion are also observed; e.g., the  $n = 8$  member of the series converging to  $X^2\Sigma^+$ ,  $v^+ = 1$  is observed at 883.58 Å.<sup>24</sup> Even though most of the observed structure is broader than the instru-

mental resolution, the present liquid nitrogen temperature spectrum shows considerably more detail than the room temperature spectrum taken at the same wavelength resolution<sup>25</sup>; this results from the narrowing of the bands due to rotational cooling. The present relative photoionization cross section can be normalized by using the absolute total photoionization data of Samson and Gardner<sup>26</sup> obtained at 28 wavelengths in the region from 304–745 Å using narrow band line sources.

### B. Vibrational branching ratios and photoelectron angular distributions

Vibrational branching ratios and photoelectron angular distributions were determined in the region 660–740 Å (16.75–18.75 eV) using the 2 m near normal incidence monochromator<sup>27</sup> at the Synchrotron Ultraviolet Radiation Facility at the National Bureau of Standards. For these measurements, the monochromator was operated with a resolution of 0.67 Å (0.017 eV at 700 Å). The electron spectrometer system<sup>28</sup> consists of two hemispherical analyzers (10.2 cm mean radius) that operate simultaneously at observation angles of 0° and 90° relative to the major polarization axis of the photon beam. Each analyzer employs a position sensitive detector at the exit plane of the hemi-

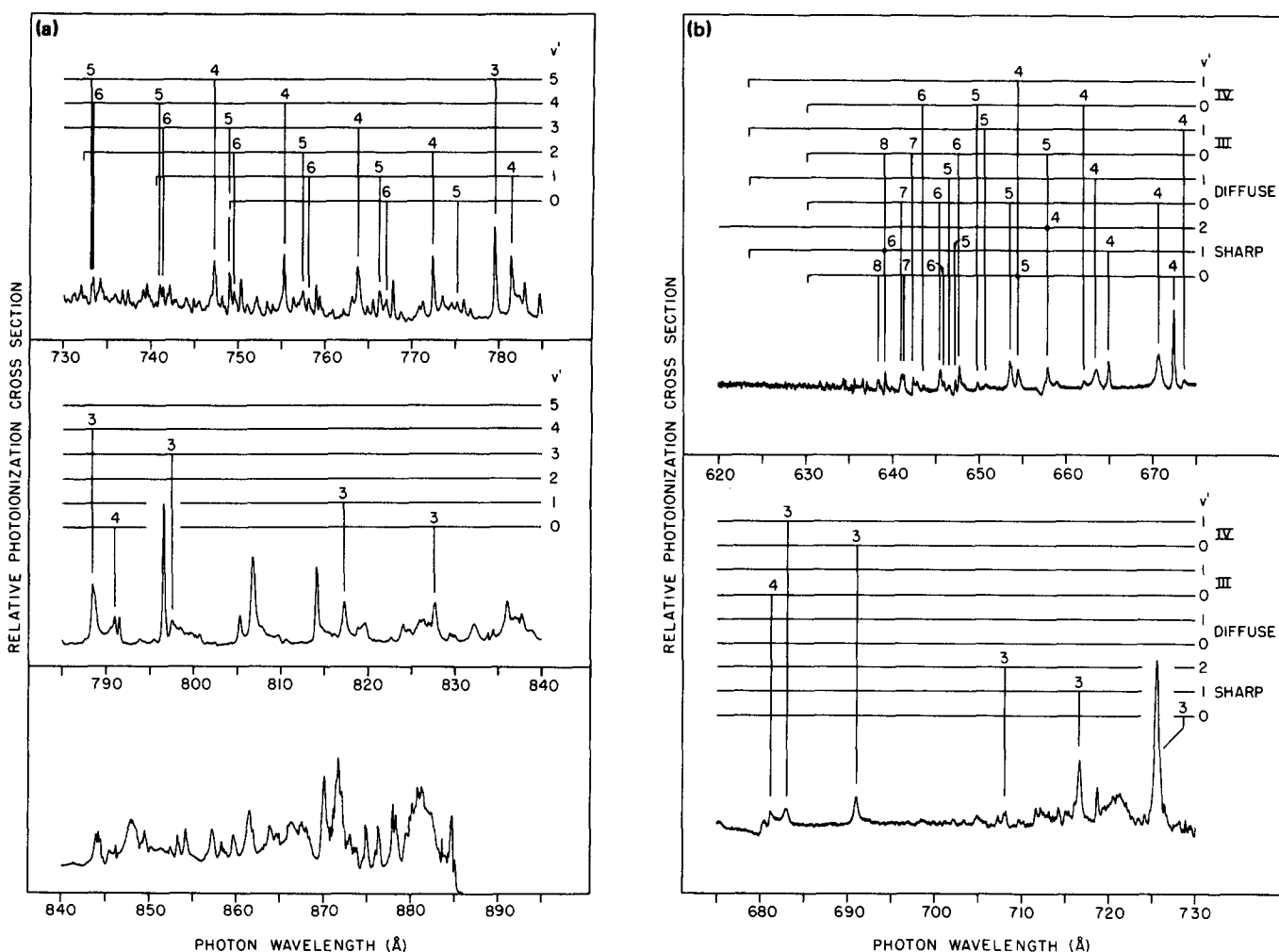


FIG. 1. Relative photoionization cross section for CO determined at a wavelength resolution of 0.07 Å and at a temperature of 78 K. Assignments are from Ogawa and Ogawa (Ref. 24) and are discussed in the text.

spheres to increase sensitivity by simultaneously detecting a range of electron energies. Photoelectron spectra were recorded in such a way that each region of the position sensitive detectors was exposed to every electron energy, thus eliminating any possible nonuniformity of response. The ionization region and the entire photoelectron flight path were shielded from magnetic and electric fields. The spectrometers were operated with a 5 eV pass energy, which resulted in an electron kinetic energy resolution of  $\sim 0.060$  eV; the combined resolution of the monochromator and electron spectrometer was easily able to resolve the vibrational components of the CO  $X^2\Sigma^+$  band. The background pressure in the vacuum chamber was  $\sim 1.4 \times 10^{-5}$  Torr, and the pressure in the ionization region was estimated to be  $\sim 10$ – $100$  times higher. These pressures produced no effect on the ratio of intensities at the two observation angles.

The differential cross section for photoionization of a randomly oriented target in the dipole approximation is

$$\frac{d\sigma}{d\Omega} = \left( \frac{\sigma_{\text{TOT}}}{4\pi} \right) \left[ 1 + \left( \frac{\beta}{4} \right) (1 + 3p \cos 2\theta) \right], \quad (1)$$

where  $\sigma_{\text{TOT}}$  is the total photoionization cross section,  $\beta$  is the asymmetry parameter,  $p = (I_{\parallel} - I_{\perp}) / (I_{\parallel} + I_{\perp})$  is the polarization of the light, and  $\theta$  is the photoelectron ejection angle relative to the major polarization axis of the light. In the present experiment, photoelectron spectra were measured at two angles, yielding

$$\frac{I(\theta_1)}{I(\theta_2)} = c \frac{[1 + (\beta/4)(1 + 3p \cos 2\theta_1)]}{[1 + (\beta/4)(1 + 3p \cos 2\theta_2)]}. \quad (2)$$

The determination of  $\beta$  and the vibrational branching ratios required several steps. First, the instrument was calibrated by determining the transmission functions for the electron spectrometers, the polarization  $p$ , and the angular correction factor  $c$ . The transmission functions characterize the detection efficiencies of the electron spectrometers as a function of incident kinetic energy. The angular correction factor represents the relative efficiencies of the electron spectrometers at the two observation angles, and it is typically within a few percent of unity; deviation from unity results from lack of cylindrical symmetry of the ionization volume due to the intersection of a diffuse gas source and a flat horizontal light beam and from other minor differences at the two angles. The determination of  $p$ ,  $c$ , and the transmission functions via measurements on He, Ar, Kr, and Xe has been described elsewhere.<sup>29,30</sup> Second, photoelectron spectra were simultaneously measured as a function of wavelength at the two observation angles and were corrected for the transmission functions of the electron analyzers to yield the quantities  $I(0^\circ)$  and  $I(90^\circ)$ . Third, the photoelectron spectra were resolved into vibrational components using nonlinear data-fitting techniques that employed Gaussian peak shapes. Fourth, the values of  $I(0^\circ)$  and  $I(90^\circ)$  for each vibrational component were combined with values of  $c$  and  $p$  to determine  $\beta$  according to Eq. (2). Finally, following the determination of  $\beta$  for each vibrational component, the vibrational branching ratios were determined from the angle independent vibrational intensities obtained by eliminating the  $\beta$  dependence from Eq. (1).

The vibrational branching ratios (and hence the  $\beta$  measurements) were wavelength calibrated by aligning the sharp features in the branching ratio curves with the known positions of the corresponding members of the Sharp series converging to the  $B^2\Sigma^+$  state of the ion.<sup>24</sup> This is an approximation, since the shapes and widths of even relatively narrow features may differ between the total cross section and the branching ratio curves. In an earlier study, Ederer *et al.*<sup>21</sup> concluded that the extrema of the 17.09 eV feature in the branching ratio curves and the relative photoionization cross section curve were offset by 0.009 eV; however, resonance line data by Samson and Gardner<sup>26,31</sup> suggested that the deviation was smaller.

### III. RESULTS AND DISCUSSION

#### A. Spectroscopic background: Classification and assignment of Rydberg series converging to $\text{CO}^+ A^2\Pi$ and $B^2\Sigma^+$

Figure 1(a) shows the high resolution photoionization cross section of CO in the region 730–885 Å (14.0–17.0 eV). This region contains Rydberg series converging to the  $A^2\Pi$  state of the ion. This region of the spectrum was first studied by Henning,<sup>32</sup> who classified two progressions [ $H(1)$  and  $H(2)$ ] and by Tanaka,<sup>33</sup> who classified three progressions [ $P(1)$ – $P(3)$ ] and one weak Rydberg series consisting of three vibrational series. Huffman *et al.*<sup>34</sup> subsequently cataloged a number of additional unclassified bands. Nearly 40 years after Henning's first work, Ogawa and Ogawa<sup>24</sup> reanalyzed this region of the spectrum and reclassified the Henning and Tanaka progressions first into a number of new progressions and then into five Rydberg series, each of which consisted of several vibrational series. One series of high intensity (denoted the  $R_A$ -I series) consisting of eight vibrational series was reported and is shown in part in Fig. 1(a). Most of the  $H(1)$ ,  $P(1)$ , and  $P(3)$  progressions were reclassified as the  $n = 3, 4,$  and  $6$  members of the  $R_A$ -I series, respectively. As is seen from Fig. 1(a), the series members are severely overlapped for  $n > 4$ , making the spectrum extremely complicated. Ogawa and Ogawa<sup>24</sup> noted that the quantum defect of this series is 0.05, which suggested the electron configuration  $(1\pi)^3 n d \lambda$ . They also noted that if the quantum defect were actually 1.05, then the electron configuration would be  $(1\pi)^3 n s \sigma$ ; however, this would require a lower series member at approximately 960 Å, and no such series member could be unambiguously identified.

Very recently, Leyh *et al.*<sup>20</sup> reassigned the series converging to the  $A^2\Pi$  state in the context of a larger work in which new measurements of the vibrationally resolved partial photoionization cross sections were reported. *Ab initio* calculations were made of the energies (and also of the vibrational cross sections) of the first members of the Rydberg series converging to  $A^2\Pi$  by using the method developed by Lefebvre-Brion<sup>35</sup> and described in detail for the application to CO by Leyh and Raseev.<sup>19</sup> Six Rydberg series were calculated corresponding to  $n s \sigma$ ,  $n p \sigma$ ,  $n p \pi$ ,  $n d \sigma$ ,  $n d \pi$ , and  $n d \delta$  transitions. Because of the strong mixing of the quasidegenerate  $(n+1)s\sigma$  and  $n d \sigma$  states, the states were actually labeled  $[(n+1)s \pm n d] \sigma$ . The precise mixing coefficients

were not reported for the series converging to the  $A^2\Pi$  state. This mixing, which is quite common in molecules such as NO and  $N_2$ , was first discussed by Jungen.<sup>36</sup> The results of the calculations showed that the  $[(n+1)s + nd]\sigma$ ,  $nd\pi$ , and  $nd\delta$  series are strong and dominate the spectrum and that the  $np\sigma$ ,  $np\pi$ , and  $[(n+1)s - nd]\sigma$  series are weak. In particular, the  $n = 3$  and  $n = 4$  members of the Ogawa and Ogawa  $R_A$ -I series were found to correspond to the  $3d\delta$  and  $4d\delta$  transitions, respectively. As noted above, the spectrum becomes quite complicated for  $n > 4$ . Not surprisingly, the higher members of the series reported by Ogawa and Ogawa<sup>24</sup> do not correspond exactly to the higher members of the calculated  $nd\delta$  series; however, it is clear that the lower members of these series are unambiguously  $nd\delta$ . The  $[(n+1)s + nd]\sigma$  series is also intense and appears prominently in the spectrum. In particular, the  $(4s + 3d)\sigma$  state corresponds to Henning's  $P(2)$  progression; the most intense member of this progression (the  $v' = 4$  member) appears at 796.55 Å and is one of the most intense transitions in this region of the spectrum. The  $nd\pi$  series is calculated to be very intense, but broad; hence, it does not appear as a series of sharp transitions, but instead modulates the background. Numerous bands in this region remain unassigned, particularly those above 840 Å.

Figure 1(b) shows the high resolution photoionization cross section of CO in the region 620–730 Å (17.0–20.0 eV). The majority of the structure in this region is Rydberg series converging to the  $B^2\Sigma^+$  state of ion; however, a particularly interesting region is that from 710–730 Å (discussed in greater detail below), where the higher members of the series converging to the  $A^2\Pi$  state interact with lowest members of the series converging to the  $B^2\Sigma^+$  state. The region of the spectrum shown in Fig. 1(b) was first studied by Tanaka,<sup>33</sup> who identified two series (Sharp and Diffuse) converging to the  $B^2\Sigma^+$  state. Later Ogawa<sup>37</sup> identified two additional series ( $R_B$ -III and  $R_B$ -IV). Ogawa and Ogawa<sup>24</sup> summarized these series and identified a few members of a fifth series ( $R_B$ -V). The prominent members of the Sharp, Diffuse, III, and IV series are shown in Fig. 1(b). Experimental evidence for the assignment of the electronic configurations of these series is scanty. In particular, rotational structure is not observed, thus prohibiting definitive assignments. However, Ogawa and Ogawa<sup>24</sup> observed that the  $n = 4$  member of the Sharp series shows a double-headed structure, which they believed was due to the  $R$  and  $Q$  bandheads; therefore, they tentatively assigned the upper levels of these transitions as  $np\pi^1\Pi$  states. Series V rapidly approaches the Sharp series as  $n$  increases, and Ogawa and Ogawa<sup>24</sup> assigned the upper levels of these transitions as the triplet series having the same electron configuration as the Sharp series.

Leyh and Raseev<sup>19</sup> have summarized previous theoretical assignments of these Rydberg series and have noted the controversy surrounding these assignments. In the first of their calculations of electronic autoionization of the Rydberg series converging to the  $B^2\Sigma^+$  state, they combined *ab initio* electronic quantities with MQDT to calculate vibrationally resolved partial and total photoionization cross sections. As in the calculation of Leyh *et al.*<sup>20</sup> of the Rydberg series converging to the  $A^2\Pi$  state of the ion,  $np\sigma$ ,  $np\pi$ ,  $nd\pi$ ,

$nd\delta$ , and  $[(n+1)s \pm nd]\sigma$  transitions were calculated. The results indicate that for the Rydberg series converging to the  $B^2\Sigma^+$  state, the most intense spectral features correspond to  $np\sigma$  and  $np\pi$  transitions, which are forbidden in the closely related homonuclear molecule  $N_2$ .<sup>13</sup> In particular, the Sharp series corresponds to the  $np\pi$  transitions (in agreement with the assignment of Ogawa and Ogawa<sup>24</sup>), and the Diffuse series corresponds to  $np\sigma$  transitions. Series III corresponds to the nearly degenerate  $nd\pi$  and  $[(n+1)s - nd]\sigma$  transitions. (Note the complex pattern of the structure at 681 Å that was assigned by Ogawa and Ogawa<sup>24</sup> as the  $n = 4$ ,  $v' = 0$  member of series III; this complex structure is indicative of a transition to more than one state.) Finally, series IV corresponds to the  $[(n+1)s + nd]\sigma$  transitions.

One of the most complex regions of the spectrum is that in the range 710–730 Å (17.0–17.5 eV); an expanded plot of this region is shown in Fig. 2. Three prominent spectral features are observed. The lowest energy feature is the intense peak at 725.51 Å (17.09 eV) assigned by Ogawa and Ogawa<sup>24</sup> as the  $n = 3$ ,  $v' = 0$  member of the Sharp series. The next feature is the broad peak (FWHM  $\approx 3$  Å) centered at  $\sim 721$  Å (17.2 eV). Considerable fine structure is superimposed on this broad feature, and a number of these weak peaks were assigned by Ogawa and Ogawa<sup>24</sup> to Rydberg states converging to  $A^2\Pi$ ,  $v^+ = 4$ , and  $v^+ = 5$ . Many weak peaks remain unassigned, some of which must be the higher- $n$  members of the Rydberg series converging to  $A^2\Pi$ ,  $v^+ = 4$  at 717.04 Å. Finally, the sharp feature at 716.60 Å (17.30 eV) was assigned by Ogawa and Ogawa<sup>24</sup> as the  $n = 3$ ,  $v' = 1$  member of the Sharp series; later Leyh and Raseev<sup>19</sup> showed that the  $n = 3$ ,  $v' = 0$  member of the Diffuse series also contributes to this peak. The current calculations of Leyh and Raseev<sup>22</sup> show that the peaks at 725.51 and 716.60 Å are complex resonances resulting from the interactions of series

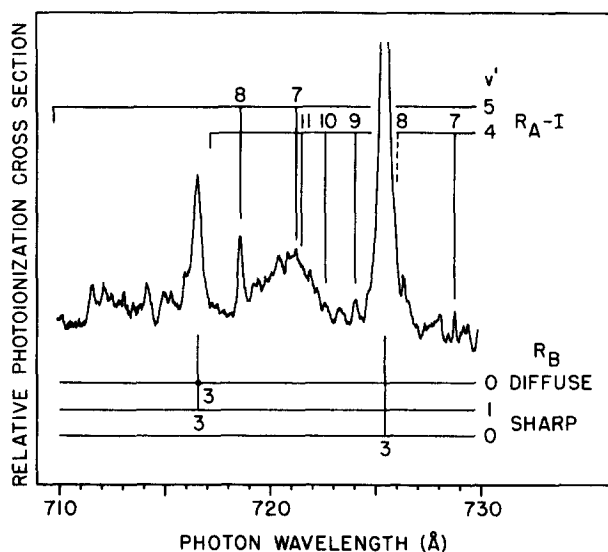


FIG. 2. Expanded view of the relative photoionization cross section for CO in the region 710–730 Å determined at a wavelength resolution of 0.07 Å and at a temperature of 78 K. Assignments are from Ogawa and Ogawa (Ref. 24).

converging to the  $A^2\Pi$  and  $B^2\Sigma^+$  states. The broad peak at 721 Å also appears in these calculations as a superposition of a number of Rydberg states; the prime contributors to the peak are Rydberg states converging to  $A^2\Pi, v^+ = 4$  as suggested by Ogawa and Ogawa. (See Ref. 22 for a discussion of the origin of this broad feature.) Still unexplained is the unusually large intensity of the  $n = 8, v' = 5$  (718.64 Å) member of the series converging to  $A^2\Pi, v^+ = 5$ .

### B. Vibrational branching ratios

A major consequence of autoionization in molecules is the redistribution of intensities among vibrational ionization channels relative to that observed in direct ionization. This redistribution is a detailed probe of autoionization dynamics; thus, the vibrational branching ratios provide an excellent test of the quality of computational approaches. The observed vibrational branching ratios for the production of  $\text{CO}^+ X^2\Sigma^+, v^+ = 0-2$  in the range 16.75–18.75 eV are shown in Fig. 3. Here the branching ratio is defined as the ratio of the angle-integrated intensity for a vibrational level to the sum of the intensities of the  $v^+ = 0-2$  levels. Since the intensities of the  $v^+ \geq 3$  levels were not recorded, some photoelectron intensity is not accounted for. The intensities of the  $v^+ \geq 3$  levels will be negligibly small in the region between autoionizing resonances, but may be larger on autoionizing resonances. Typical error bars are shown on the lowest energy data points of each branching ratio spectrum; the error bars extend beyond the symbol used for the data only for  $v^+ = 0$ . The top frame of Fig. 3 shows the relative photoionization cross section of Fig. 1 on the same energy scale as the branching ratio spectra, and the positions of the  $\text{CO}^+ A^2\Pi, v^+ = 1-7$  ionization thresholds<sup>24</sup> are noted above the spectrum. Also included in Fig. 3 is the two-step MQDT calculation by Leyh and Raseev<sup>22</sup> convoluted with the instrumental resolution of 0.017 eV (solid lines).

The autoionization structure in the photoionization cross section is clearly reflected in the branching ratio spectra of Fig. 3. In particular, the resonances at 17.09, 17.2, and 17.30 eV are observed in the three vibrational channels, although the 17.2 eV resonance is very weak in the  $v^+ = 1$  channel, as is discussed below. The most obvious effect of autoionization is the shift of intensity from the intense  $v^+ = 0$  channel into the weaker  $v^+ = 1$  and  $v^+ = 2$  channels relative to the direct photoionization intensity distribution.

This redistribution of vibrational intensities can be understood in very simple terms. To a first approximation, the vibrational intensities for direct photoionization are proportional to the Franck–Condon factors between the initial state and the final ionic state. Smith<sup>38</sup> first pointed out an intuitive modification to this approximation for electronic autoionization of high- $q$  resonances. In this case, the vibrational intensities for autoionization are proportional to the Franck–Condon factors between the quasibound intermediate state and final ionic state. We stress that these simple ideas have long been superseded by more exact theories of autoionization. Nevertheless, the simple Franck–Condon arguments are often useful for a preliminary interpretation of data.

As an example of direct ionization, we consider ioniza-

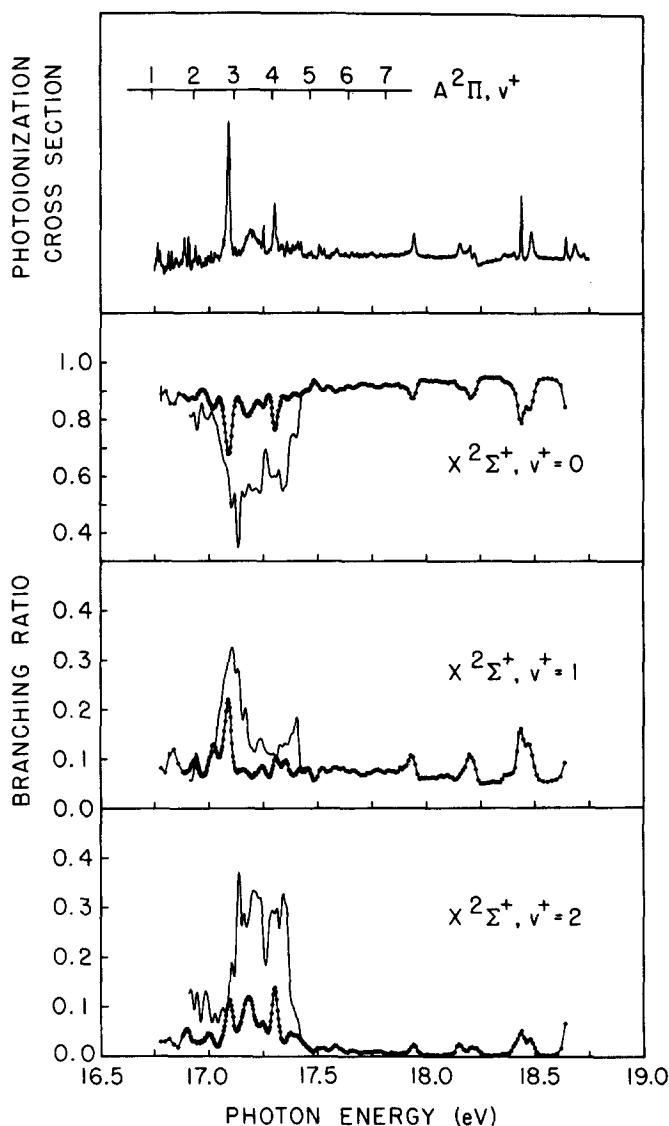


FIG. 3. Relative photoionization cross section of CO (top frame) and vibrational branching ratios for  $\text{CO}^+ X^2\Sigma^+, v^+ = 0-2$  produced by photoionization of  $\text{CO } X^1\Sigma^+, v'' = 0$ . The solid curves in the lower three frames are the theoretical results of Leyh and Raseev (Ref. 22), convoluted with the experimental resolution of 0.017 eV. The ionization thresholds (Ref. 24) for  $\text{CO}^+ A^2\Pi, v^+ = 1-7$  production are shown in the top frame.

tion of  $\text{CO } X^1\Sigma^+, v'' = 0$  to produce  $\text{CO}^+ X^2\Sigma^+, v^+$ . The branching ratios calculated from the Franck–Condon factors for direct ionization are  $\sim 0.96$  ( $v^+ = 0$ ) and  $\sim 0.04$  ( $v^+ = 1$ ),<sup>39</sup> which are very close to the observed values of  $\sim 0.95$  ( $v^+ = 0$ ) and  $\sim 0.05$  ( $v^+ = 1$ ) obtained in regions where the effects of autoionization are minimal.

As examples of resonant cases, we consider the autoionizing features at 17.09, 17.2, and 17.30 eV. The resonance at 17.09 eV is a mixture of the  $3p\pi, v' = 0$  Rydberg state converging to  $B^2\Sigma^+$  (the dominant contribution to the resonance), high- $n$  members of Rydberg series converging to  $A^2\Pi$ , and the underlying  $X^2\Sigma^+$  continuum. Since the resonance is dominated by the  $3p\pi, v' = 0$  state, the Franck–Condon factors between this state and the  $X^2\Sigma^+, v^+$  levels provide the initial approximation to the branching ratios. Assuming that the  $3p\pi$  Rydberg state has a potential energy

curve identical to that of the  $\text{CO}^+ B^2\Sigma^+$  state to which it converges, the resulting branching ratios determined from the Franck–Condon factors are 0.55 ( $v^+ = 0$ ), 0.35 ( $v^+ = 1$ ), and 0.10 ( $v^+ = 2$ ).<sup>22</sup> The corresponding experimental values are 0.68 ( $v^+ = 0$ ), 0.22 ( $v^+ = 1$ ), and 0.10 ( $v^+ = 2$ ). Considering the level of approximation and the neglect of the nonresonant background, this is satisfactory agreement, although higher resolution might well improve the agreement by increasing the magnitudes of the dip in the  $v^+ = 0$  branching ratio spectrum and of the peak in the  $v^+ = 1$  branching ratio spectrum. This resonance was previously studied by Ederer *et al.*,<sup>21</sup> who obtained branching ratios of 0.75 ( $v^+ = 0$ ), 0.18 ( $v^+ = 1$ ), and 0.07 ( $v^+ = 2$ ) using a wavelength resolution of 0.8 Å and by Samson and Gardner,<sup>26,31</sup> who obtained branching ratios of 0.61 ( $v^+ = 0$ ), 0.25 ( $v^+ = 1$ ), and 0.14 ( $v^+ = 2$ ) using a narrow band line source. These results are all in reasonable agreement, and the variations correlate with wavelength resolution in a logical way.

Since the main contributors to the broad resonance at 17.2 eV are a number of high- $n$  Rydberg states converging to  $A^2\Pi$ ,  $v^+ = 4$ ,<sup>22,24</sup> the relevant Franck–Condon factors are those between  $A^2\Pi$ ,  $v^+ = 4$  and  $X^2\Sigma^+$ ,  $v^+$ . The resulting branching ratios determined from the Franck–Condon factors are 0.61 ( $v^+ = 0$ ), 0.02 ( $v^+ = 1$ ), and 0.37 ( $v^+ = 2$ ).<sup>22</sup> The observed values of 0.81 ( $v^+ = 0$ ), 0.07 ( $v^+ = 1$ ), and 0.12 ( $v^+ = 2$ ) are in qualitative agreement with this prediction, and, in particular, the very small  $v^+ = 1$  branching ratio was correctly predicted.

The resonance at 17.30 eV is a mixture of the nearly degenerate  $3p\pi$ ,  $v' = 1$  and  $3p\sigma$ ,  $v' = 0$  Rydberg states converging to  $B^2\Sigma^+$ , high- $n$  members of Rydberg series converging to  $A^2\Pi$ , and the underlying  $X^2\Sigma^+$  continuum. The branching ratios determined from the Franck–Condon factors for decay of a Rydberg state with  $v' = 0$  converging to  $B^2\Sigma^+$  are 0.55 ( $v^+ = 0$ ), 0.35 ( $v^+ = 1$ ), and 0.10 ( $v^+ = 2$ );<sup>22</sup> the branching ratios determined from the Franck–Condon factors for decay of a Rydberg state with  $v' = 1$  converging to  $B^2\Sigma^+$  are 0.45 ( $v^+ = 0$ ), 0.09 ( $v^+ = 1$ ), and 0.46 ( $v^+ = 2$ ).<sup>22</sup> The experimental values are 0.76 ( $v^+ = 0$ ), 0.10 ( $v^+ = 1$ ), 0.14 ( $v^+ = 2$ ); the nonmonotonic variation of the branching ratios is accounted for, but, again, the complexity of the actual physical process and the failure to adjust for the effects of the nonresonant background make it inappropriate to go beyond the qualitative level.

The new theoretical results of Leyh and Raseev,<sup>22</sup> shown as the solid lines in Fig. 3, are described in detail in the companion paper and will not be discussed here. We only note that these calculations are two-step MQDT calculations that incorporate the vibrational structure of the  $X^2\Sigma^+$ ,  $A^2\Pi$ , and  $B^2\Sigma^+$  states of the ion in the Franck–Condon approximation. The calculation was a very ambitious one, incorporating 164 channels, and the solid curves shown in Fig. 3 are, in fact, hundreds of individual spectral features convoluted with the monochromator resolution of 0.017 eV.

The comparison between experiment and theory is most interesting. The calculation accounted for much of the observed behavior and revealed the nature of the three promi-

nent resonances at 17.09, 17.2, and 17.30 eV. In particular, the resonance at 17.2 eV had not appeared in the earlier calculations<sup>19</sup> that did not include the vibrational structure of the  $A^2\Pi$  state. The calculation also accounted for the resonant transfer of intensity from the strong  $v^+ = 0$  channel to the weaker  $v^+ = 1$  and 2 channels, as well as for the nonmonotonic branching ratios for the 17.2 and 17.30 eV resonances in the  $v^+ = 1$  and  $v^+ = 2$  channels. The simple Franck–Condon arguments given above could account for the latter, but did not reveal the complex nature of the resonances.

It is clear, however, that the agreement is not yet satisfactory. In some cases, the magnitudes of the branching ratios in the resonant regions are in error by more than a factor of 3, and the shapes do not reflect experiment very closely. The present level of approximation also overestimates the vibrationally summed branching ratio for the  $X^2\Sigma^+$  to  $A^2\Pi$  ion states.<sup>22,26,31,40</sup> These residual problems indicate the need to eliminate remaining approximations in the already highly ambitious treatment. For example, going beyond the Franck–Condon approximation would seem to be an important step. This would permit vibrational autoionization of the states converging to  $A^2\Pi$ ,  $v^+ > 0$ . In addition, dissociation is not negligible in this spectral range, and coupling with dissociation channels could affect the photoionization dynamics. Finally, going beyond a single configuration description of the ion cores might be necessary.

### C. Photoelectron angular distributions

A prime motivation for this work was the resolution of the disagreement between the theoretical<sup>19</sup> and experimental<sup>21</sup> photoelectron angular distribution of the  $3p\pi$ ,  $v' = 0$  resonance at 17.09 eV. Recall that at the resonance position, the theory showed a minimum, while the experiment showed a maximum. The new data, taken over a broader energy range, are shown in Fig. 4. As in Fig. 3, the top frame shows the relative photoionization cross section of Fig. 1 on the same energy scale as the angular distributions; the positions of the  $\text{CO}^+ A^2\Pi$ ,  $v^+ = 1$ –7 ionization thresholds<sup>24</sup> are noted above the spectrum. Typical error bars are shown on the lowest energy data points in each frame. Also included in Fig. 4 is the two-step MQDT calculation by Leyh and Raseev<sup>22</sup> convoluted with the instrumental resolution of 0.017 eV (solid lines). The data near the 17.09 eV resonance agree well with the earlier measurement by Ederer *et al.*<sup>21</sup>

Comparison of the photoionization cross section and asymmetry parameter data in Fig. 4 graphically demonstrates that autoionization structure is not as easily identified in the  $\beta$  curves as it is in the branching ratio curves. The interference terms in the expression for  $\beta$  complicate and effectively broaden the response of  $\beta$  to resonances. As a result, the resonance profiles in the  $\beta$  curves are generally much broader than the resonance half-widths, and resonances that appear as isolated features in the total photoionization cross section are blended in the  $\beta$  curves. This is clearly shown in the high energy region of the middle two frames in Fig. 4. Thus, the resonance profile in the  $\beta$  curves rarely gives a clear indication of the resonance position, and only in

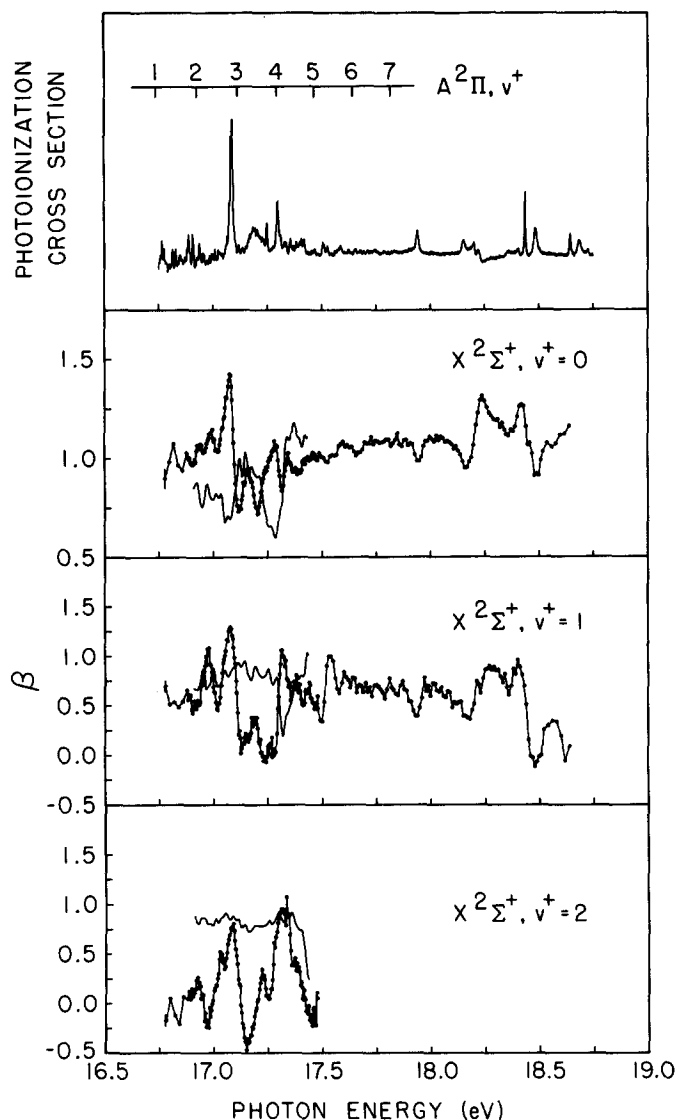


FIG. 4. Relative photoionization cross section of CO (top frame) and photoelectron asymmetry parameters for  $\text{CO}^+ X^2\Sigma^+, v^+ = 0-2$  produced by photoionization of  $\text{CO } X^1\Sigma^+, v^+ = 0$ . The solid curves in the lower three frames are the theoretical results of Leyh and Raseev (Ref. 22), convoluted with the experimental resolution of 0.017 eV. The ionization thresholds (Ref. 24) for  $\text{CO}^+ A^2\Pi, v^+ = 1-7$  production are shown in the top frame.

a few cases does visual inspection suggest that a characteristic shape in  $\beta$  correlates with a particular spectral feature. For example, the data of Fig. 4 show that the  $n = 3, v^+ = 0$  and  $n = 4, v^+ = 0$  members of the Sharp series fall near peaks in the  $\beta$  curves, and the  $n = 3, v^+ = 0$  and 1 members of the series IV fall near minima in the  $\beta$  curves; however, without corresponding theoretical calculations, these data are difficult to interpret.

Thus, we consider the comparison with the new two-step MQDT calculation of Leyh and Raseev,<sup>22</sup> who have incorporated the vibrational structure of the  $X^2\Sigma^+, A^2\Pi$ , and  $B^2\Sigma^+$  states of  $\text{CO}^+$  within the Franck-Condon approximation. The unconvoluted calculation is extremely complex, exhibiting sharp Rydberg structure converging to the  $A^2\Pi$  and  $B^2\Sigma^+$  states. The unconvoluted theoretical curves vary over the range  $-0.2 < \beta < 1.7$  between 17.0 and 17.5 eV. This rich variation is effectively eliminated when

the theoretical curves are convoluted with the instrumental resolution to produce the solid curves in Fig. 4. The two generations of calculations<sup>19,22</sup> show some differences as discussed by Leyh and Raseev<sup>22</sup> in various ways including decomposition schemes by Thiel<sup>41,42</sup> and by Kabachnik and Sazhina.<sup>43</sup> Here we will concentrate only on the comparison between the convoluted results and experiment. Three points are apparent. First, the magnitude of the theory curves, when averaged over the spectral range in Fig. 4, agrees well with experiment for the more intense  $v^+ = 0$  and  $v^+ = 1$  channels. As discussed by Leyh and Raseev,<sup>22</sup> this is a nontrivial result. Second, as in the earlier comparison between the first generation calculation and the experiment by Ederer *et al.*,<sup>21</sup> theory and experiment do not agree in the immediate vicinity of the 17.09 eV resonance. Specifically, the experiment shows a maximum near the resonance in the  $v^+ = 0$  channel, while the calculation shows a minimum. Third, considering the entire 17.0–17.5 eV spectral range, one must conclude that the agreement between theory and experiment remains unsatisfactory despite the recent improvements in the theory. This may arise from the causes briefly mentioned at the end of the last section, but, in any case, it is obvious that the agreement between theory and experiment for the angular distributions is much poorer than it is for the branching ratios. Thus, the angular distributions may be a more discriminating test for future improvements in the theoretical approach.

#### IV. SUMMARY AND CONCLUSIONS

We have presented detailed measurements of photoionization cross sections, vibrational branching ratios, and photoelectron angular distributions in the vicinity of complex autoionization structure in the valence-shell photoionization spectrum of CO. High resolution photoabsorption and photoionization measurements have been relatively routine for many years; however, angle-resolved photoelectron studies of autoionization at good resolution ( $\Delta\lambda < 1 \text{ \AA}$ ) and with variable wavelength are of more recent advent. The present study of CO is a good example of the resolution and data quality that can now be achieved. This study was done in parallel with the two-step MQDT calculations by Leyh and Raseev.<sup>22</sup> The combined results provided a much greater understanding of the nature of the resonant structures below 20 eV and achieved at least qualitative understanding of many aspects of the vibrational branching ratios. However, the present state of our understanding of the photoelectron angular distributions was demonstrated to be unsatisfactory.

This study clearly demonstrated the need for coordinated experimental and theoretical efforts to advance the understanding of molecular photoionization dynamics into a broader range of molecules, starting with first row diatomics. The nature of needed improvements was also emphasized. On the experimental side, higher photon resolution is critical in order to minimize the loss of information typified by the convolution of theoretical results used in this work. On the theory side, essential physics must be retained by eliminating simplifying assumptions such as the Franck-

Condon separation and single configuration representations currently needed to make multichannel calculations tractable.

## ACKNOWLEDGMENTS

We wish to thank the staff at NBS SURF for their cooperation during these measurements. This work was supported in part by the U.S. Department of Energy, Office of Health and Environmental Research, under Contract No. W-31-109-Eng-38, and by the National Science Foundation under Grant No. CHE-8318419.

- <sup>1</sup>J. L. Dehmer, A. C. Parr, and S. H. Southworth, in *Handbook of Synchrotron Radiation*, edited by G. V. Marr (North-Holland, Amsterdam, 1987), Vol. II, p. 241.
- <sup>2</sup>I. Nenner and J. A. Beswick, in *Handbook of Synchrotron Radiation*, edited by G. V. Marr (North-Holland, Amsterdam, 1987), Vol. II, p. 355.
- <sup>3</sup>C. H. Greene and Ch. Jungen, in *Advances in Atomic and Molecular Physics* (Academic, New York, 1985), Vol. 21, p. 51.
- <sup>4</sup>G. Raseev, B. Leyh, and H. Lefebvre-Brion, *Z. Phys. D* **2**, 319 (1986).
- <sup>5</sup>D. Dill and Ch. Jungen, *J. Phys. Chem.* **84**, 2116 (1980).
- <sup>6</sup>Ch. Jungen and D. Dill, *J. Chem. Phys.* **73**, 3338 (1980).
- <sup>7</sup>Ch. Jungen, *J. Chim. Phys.* **77**, 27 (1980).
- <sup>8</sup>Ch. Jungen and M. Raoult, *Faraday Discuss. Chem. Soc.* **71**, 253 (1981).
- <sup>9</sup>C. Cornaggia, A. Giusti-Suzor, and Ch. Jungen, *J. Chem. Phys.* **87**, 3934 (1987).
- <sup>10</sup>M. Raoult, Ch. Jungen, and D. Dill, *J. Chim. Phys.* **77**, 599 (1980).
- <sup>11</sup>M. Raoult and Ch. Jungen, *J. Chem. Phys.* **74**, 3388 (1981).
- <sup>12</sup>Ch. Jungen, *Phys. Rev. Lett.* **53**, 2394 (1984).
- <sup>13</sup>M. Raoult, H. LeRouzo, G. Raseev, and H. Lefebvre-Brion, *J. Phys. B* **16**, 4601 (1983).
- <sup>14</sup>H. Lefebvre-Brion, A. Giusti-Suzor, and G. Raseev, *J. Chem. Phys.* **83**, 1557 (1985).
- <sup>15</sup>H. Lefebvre-Brion, P. M. Dehmer, and W. A. Chupka, *J. Chem. Phys.* **85**, 45 (1986).
- <sup>16</sup>H. Lefebvre-Brion, P. M. Dehmer, and W. A. Chupka, *J. Chem. Phys.* **88**, 811 (1988).
- <sup>17</sup>A. Giusti-Suzor and H. Lefebvre-Brion, *Chem. Phys. Lett.* **76**, 132 (1980).
- <sup>18</sup>A. Giusti-Suzor and Ch. Jungen, *J. Chem. Phys.* **80**, 986 (1984).
- <sup>19</sup>B. Leyh and G. Raseev, *Phys. Rev. A* **34**, 2920 (1986).
- <sup>20</sup>B. Leyh, J. Delwiche, M.-J. Hubin-Franskin, and I. Nenner, *Chem. Phys.* **115**, 243 (1987).
- <sup>21</sup>D. L. Ederer, A. C. Parr, B. E. Cole, R. Stockbauer, J. L. Dehmer, J. B. West, and K. Codling, *Proc. R. Soc. London Ser. A* **378**, 423 (1981).
- <sup>22</sup>B. Leyh and G. Raseev, *J. Chem. Phys.* **89**, 820 (1988).
- <sup>23</sup>W. A. Chupka, P. M. Dehmer, and W. T. Jivery, *J. Chem. Phys.* **63**, 3929 (1975).
- <sup>24</sup>M. Ogawa and S. Ogawa, *J. Mol. Spectrosc.* **41**, 393 (1972).
- <sup>25</sup>J. Berkowitz, *Photoabsorption, Photoionization, and Photoelectron Spectroscopy* (Academic, New York, 1979), p. 228.
- <sup>26</sup>J. A. R. Samson and J. L. Gardner, *J. Electron Spectrosc. Relat. Phenom.* **8**, 35 (1976).
- <sup>27</sup>D. L. Ederer, B. E. Cole, and J. B. West, *Nucl. Instrum. Methods* **172**, 185 (1980).
- <sup>28</sup>A. C. Parr, S. H. Southworth, J. L. Dehmer, and D. M. P. Holland, *Nucl. Instrum. Methods* **222**, 221 (1984).
- <sup>29</sup>S. H. Southworth, A. C. Parr, J. E. Hardis, J. L. Dehmer, and D. M. P. Holland, *Nucl. Instrum. Methods A* **246**, 782 (1986).
- <sup>30</sup>A. C. Parr, J. E. Hardis, S. H. Southworth, C. S. Feigerle, T. A. Ferrett, D. M. P. Holland, F. M. Quinn, B. R. Dobson, J. B. West, G. V. Marr, and J. L. Dehmer, *Phys. Rev. A* **37**, 437 (1988).
- <sup>31</sup>J. L. Gardner and J. A. R. Samson, *J. Electron Spectrosc. Relat. Phenom.* **13**, 7 (1978).
- <sup>32</sup>H. J. Henning, *Ann. Phys. (Paris)* **13**, 599 (1932).
- <sup>33</sup>Y. Tanaka, *Sci. Papers Instrum. Phys. Chem. Research (Tokyo)* **39**, 447 (1942).
- <sup>34</sup>R. E. Huffman, J. C. Larrabee, and Y. Tanaka, *J. Chem. Phys.* **40**, 2261 (1964).
- <sup>35</sup>H. Lefebvre-Brion, *J. Mol. Spectrosc.* **19**, 103 (1973).
- <sup>36</sup>Ch. Jungen, *J. Chem. Phys.* **53**, 4168 (1970).
- <sup>37</sup>M. Ogawa, *J. Chem. Phys.* **43**, 2142 (1965).
- <sup>38</sup>A. L. Smith, *Philos. Trans. R. Soc. London Ser. A* **268**, 169 (1970).
- <sup>39</sup>P. H. Krupenie, *The Band Spectrum of Carbon Monoxide*, Natl. Stand. Ref. Data Ser., Natl. Bur. Stand. No. 5 (U.S. GPO, Washington, D.C., 1966).
- <sup>40</sup>E. W. Plummer, T. Gustafsson, W. Gudat, and D. E. Eastman, *Phys. Rev. A* **15**, 2339 (1977).
- <sup>41</sup>W. Thiel, *Chem. Phys. Lett.* **87**, 249 (1982).
- <sup>42</sup>W. Thiel, *Chem. Phys.* **77**, 103 (1983).
- <sup>43</sup>N. M. Kabachnik and I. P. Sazhina, *J. Phys. B* **9**, 1681 (1976).